Evaluation of Single Point Incremental Forming Process for Parabolic AA6082 Cups

A. Chennakesava Reddy

Abstract— In search for new manufacturing process, Single Point Incremental Forming (SPIF) emerged to be one of the useful processes for forming complicated shapes. This is a flexible forming process which eliminates the die, punch and errors due to them. It is widely used for batch production of different shapes which has applications in diverse fields like automobile, aerospace, medical industry, packaging industry etc. The equipment requirement of SPIF process is very simple, which includes; standard 3-axis CNC machine, a rotating spherical or hemispherical tool and a clamping setup. The SPIF is a sheet metal forming technique where a sheet is deformed locally. The forming of sheet due to a series of local deformation increases the formability of the sheet, when compared to conventional sheet forming process. The present work was to study the formability of parabolic cup on AA6082 sheet using SPIF process. For validating the results of simulation, a parabolic cup was drawn on AA6082 sheet using SPIF process on a CNC machine. The deformed patterns of grid on formed cups from experimentation were similar to that of deformed pattern of mesh in simulated cups from FEA. The experimental strains of the formed cups were within the forming limits, as there was no fracture observed.

Index Terms— AA6082 alloy, incremental forming process, parabolic cups.

1 Introduction

SINGLE Point Incremental Forming (SPIF) is a new metal forming process with a high potential economic pay off for rapid prototyping applications suitable for flexible and small quantity batch production fulfilling the gaps in metal forming process. The SPIF includes the local deformation of the sheet blank using simple spherical or hemispherical tool. The tool is mounted on to a simple CNC machine having three degrees of freedom (X, Y and Z axis). A tool path is then decided and moved accordingly over the sheet with vertical feed. As no die is used for any kind of complicated shapes it is called 'die less' process. Due to its low-cost production setup, along with CNC machine, this method is proving to be flexible one. Adoption of 6-axes robots or hybrid ISF can further increase the flexibility of the process.

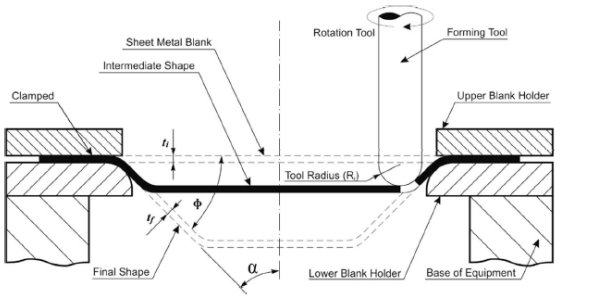

Fig. 1. Single point incremental forming.

The techniques adopted for sheet metal operations in the olden days were pressing, spinning and deep drawing. In a series of research on deep drawing process, a rich investigation have been carried out on warm deep drawing process to improve the super plastic properties of materials such as AA1050 alloy [1], [2], [3], [4], [5,] [6], AA2014 alloy [7], AA2017 alloy [8], AA2024 alloy [9], AA2219 alloy [10], AA2618 alloy [11], AA3003 alloy [12], AA5052 alloy [13], AA5049 alloy [14], AA5052 alloy [15], AA6061 alloy [16], Ti-Al-4V alloy [17], EDD steel [18], gas cylinder steel [19].

The SPIF may seem to be simple, but it is heavily influenced by different process parameters. It is influenced by parameters like tool Path, sheet material, forming angle, tool size, step size, forming speeds (rotation and feed rate), lubrication, and shape [20], [21].

Azauzi et al. [22] have worked on tool path optimization for single point incremental sheet forming using response surface methodology. They have found that the forming forces depend largely on the proper design of the tool path. ISF process depends strongly on the forming tool path which influences greatly the part geometry and sheet thickness distribution. They also suggested that a homogeneous thickness distribution requires a rigorous optimization of the parameter settings, and an optimal parameterization of the forming strategy.

Filice et al. [23] proposed the two characteristics of deformation in this forming method. One is the deformation pattern. While the tool moves straight on a horizontal plane, the deformation that occurs at the starting and ending points of the straight line is biaxial stretching. The deformation that occurs between these points is plane-strain stretching. As the curvature of the tool movement increases, the deformation turns more into biaxial stretching. The other characteristic is the formability of the deformation.

Thibaud et al. [24] worked on a fully parametric toolbox for the simulation of single point incremental sheet forming process. They have worked on single point incremental forming (SPIF) which allows sheet metal forming process that allows manufacturing components without the development of complex tools in comparison with stamping process. Their work is dedicated to the development of SPIF for microparts (shape or detail) and for thin metal sheets (less than 1mm). They have

• *Alavala Chennakesava Reddy is currently Professor & Director (Foreign Relations) in JNT University, India, Mobile-09449568776. E-mail: chennakesava@jntuh.ac.in*

formed a pyramidal shape which is 4mm in height from a copper sheet with an initial thickness of 0.21 mm.

Neto et al. [25] worked on Evaluation of strain and stress states in the single point incremental forming process. They have developed a comprehensive finite element model to analyse the state of strain and stress in the vicinity of the contact area, where the plastic deformation increases by means of the forming tool action. The numerical model was firstly validated with experimental results from a simple truncated cone of AA7075-O aluminium alloy, namely, the forming force evolution, the final thickness and the plastic strain distributions. In order to evaluate accurately the through-thickness gradients, the blank was modelled with solid finite elements.

Majagi et al. [26] have worked together on analyzing the effect of process parameters on AA1050, with the help of taguchi technique, L27 array and found that the most influencing factor was thickness of sheet.

Arfa et al. [27] worked on Finite element modelling and experimental investigation of single point incremental forming process of aluminium sheets. They have found that the highest value of the forming angle results in the largest equivalent plastic strains on the sheet surface and larger thinning.

The objective of the present work was finite element analysis of parabolic cups formed by SPIF and the same was validated experimentally.

2 Materials and Methods

Aluminum alloy 6082 was the material used for the fabrication of parabolic cups using SPIF process. AA6082 is a medium strength which has excellent corrosion strength. It has the highest strength in 6000 series. As relatively new alloy it is replacing 6061 alloy which is mostly used n aerospace industry. Material properties considered in this study as shown in Table 2 and imported to finite element analysis.

TABLE 1
Composition of AA6082 alloy

Fe	*Si*	*Mn*	*Ti*	*Cr*	*Cu*	*Mg*	*Zn*	*Al*
0.5	*0.7-1.3*	*0.4-01*	*0.1*	*0.25*	*0.1*	*0.6-1.2*	*0.2*	*Balance*

TABLE 2
Mechanical properties of AA6082 alloy

Density	*2700 kg/m³*
Young's modulus	*70 GPa*
Tensile strength	*300 MPa*
Poisson's ratio	*0.33*

The values of true stress-true strain are taken from the tension test on AA6082 alloy. Graph between stress and strain for phosphorous bronze is shown in figure 1. The obtained values were taken as material properties-plasticity for simulation of SPIF process. Graph between stress and strain for AA6082 alloy is shown in figure 1. The obtained values were taken as material properties-plasticity for simulation of SPIF process.

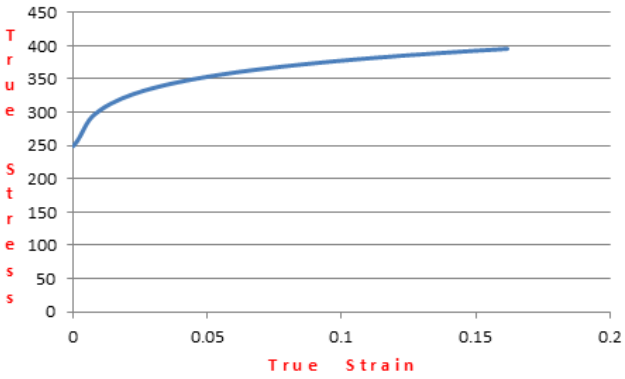

Fig. 1. True stress-strain curve of AA6082 alloy.

2.1 Numerical Pre-processing

The experimental setup is geometrically modelled. A 150mm x 150mm sheet as shown in figure 2, which is of deformable characteristic, was modelled. Tool for the experiment was designed with 6 mm radius. The tool was modelled as analytical rigid part in character. The two bodies were assembled as frictional contact bodies abiding coulomb's friction law.

The sheet is meshed with S4R elements. A 4-node doubly curved thin or thick shell, reduced integration, hourglass control, finite membrane strains are S4R elements. The Table-3 shows the quantity of elements, nodes and variables produced after meshing the sheet. Meshed part can be seen from the figure 3.

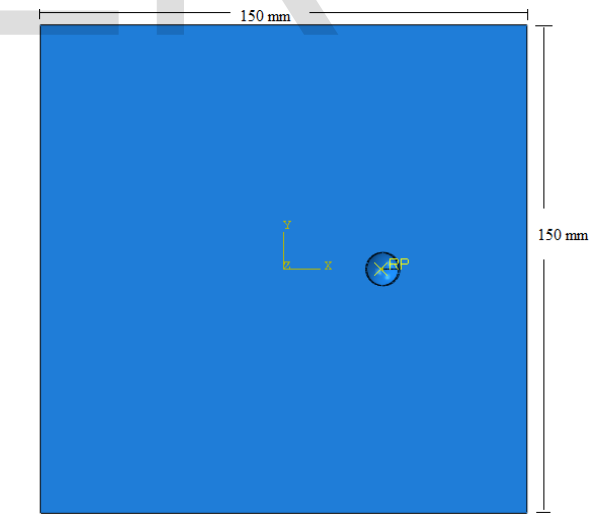

Fig. 2. Modeled sheet and Tool.

TABLE 3
Nodes and Elements

Element size	*2mm*
No. of Elements	*5625*
No. of Nodes	*5777*
Total no. of variables	*34662*

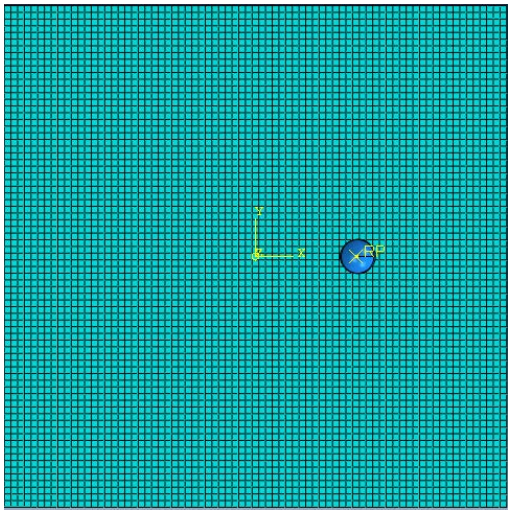

Fig. 3. Meshed sheet.

Boundary conditions for the sheet and tool were given. For the sheet, all the four edges were fixed as show in figure 4. The boundary conditions for tool were four degrees of freedom, i.e. linear movements in x, y and z directions and rotation about the axis of tool. The tool path generated from CAM software was imported into the ABAQUS code and the simulation was run to optimize the parameters.

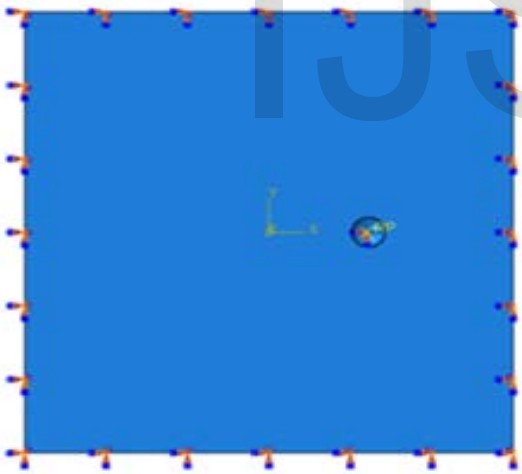

Fig. 4. Boundary conditions.

2.2 Experimental Validation

A 3-axis CNC machine is required to perform the SPIF process. The machine consists of a table on which the work holder is fixed. The table can move either along x or y axes direction. A spindle with a collect holds the tool and it can move along z axis. The tool path was generated using G-codes and M-codes. The code was fed into the CNC machine manually. The tool path generated from the code is shown in figure 5.

AA6082 sheet of 150mm x 150mm was cut from a large sheet of thickness 1mm or 1.2mm with the help of shearing bench. Holes are made in the corners of the sheet using a drilling machine (figure 6). This sheet was mounted to the worktable of the CNC machine and it became the platform for forming. The clamping and top plates restrict flange material flow into the forming region that is defined by tool path generated from the CAM software and due to this clamping restriction tool applies much localized stresses to deform the sheet. Before proceeding to the experiment a pre-check of the codes can be done with the demo option in the CNC (figure 7).

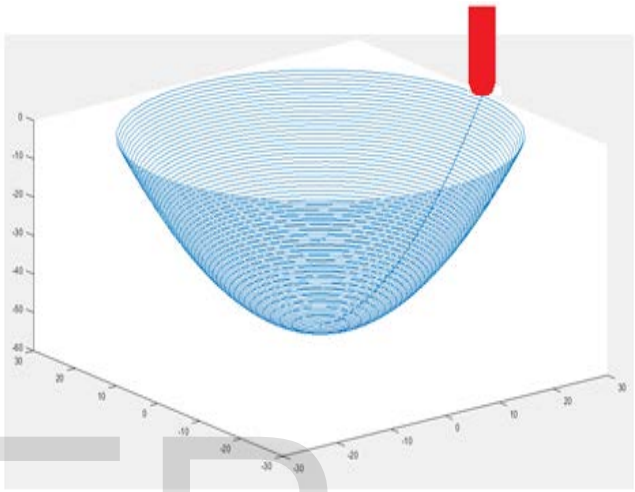

Fig. 5. Tool path generation.

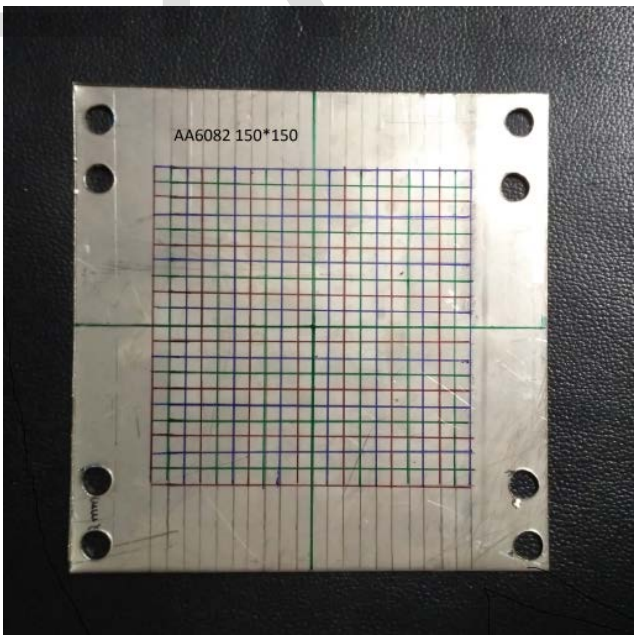

Fig. 6. Prepared sheet.

Once the operator is satisfied with the demo, the experiment can be run on the CNC. The tool position was set at the required position. Lubrication at the interface of tool and sheet was provided and the experiment was conducted. The Figure

8 illustrates the experiment on CNC for the parabolic cup.

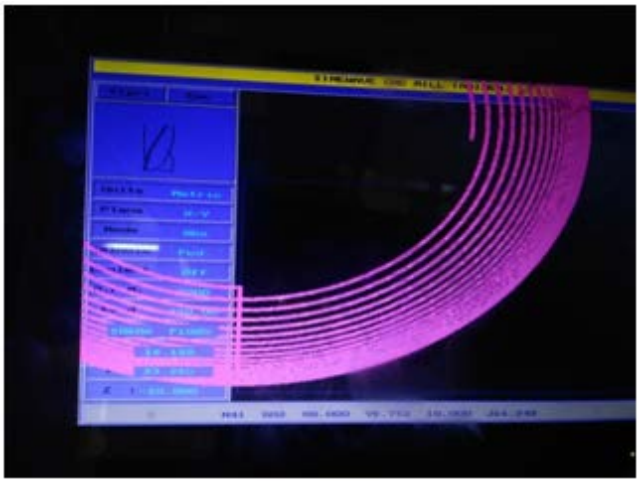

Fig. 7. Demo of CNC program on monitor screen.

Fig. 8. Forming of parabolic cup on CNC machine.

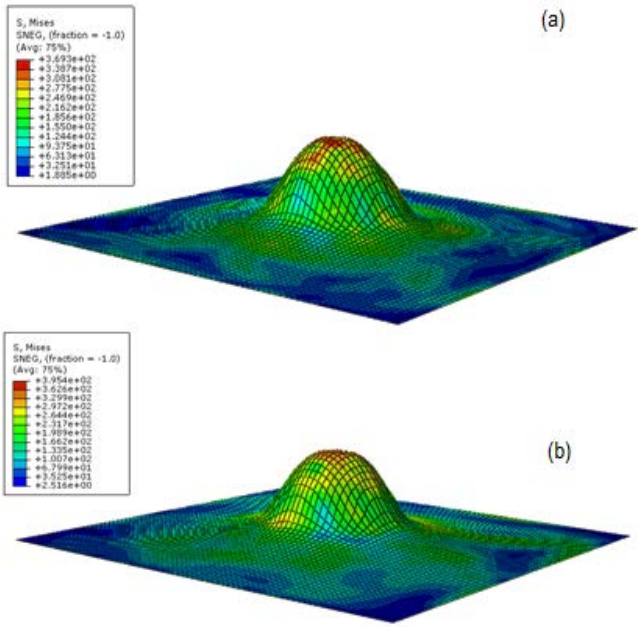

Fig. 9. Equivalent stress induced in sheet thickness of (a) 1mm and (b)1.2mm.

3 Results and Discussion

For the 1 mm and 1.5 mm cups, the maximum equivalent stress induced are, 369.3 MPa (figure 9(a)) and 395.4 MPa (figure 9(b)), respectively. For both the cups the maximum equivalent stress was found in the side walls of cups.

To validate the simulation results, the finite element grid of 5mm size was created on the backside of the cup material. The size of element was 2mm in case of simulation results. The stress pattern obtained by the finite element analysis coincides with the pattern on the cups. The stress patterns for formed cups of both 1 mm and 1.5 mm are shown in figures 10(a) and 10(b), respectively.

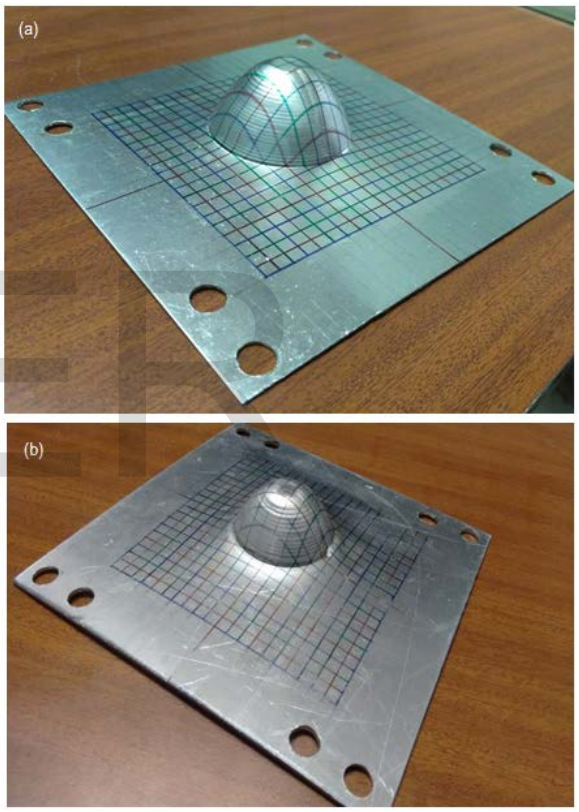

Fig. 10. Grid based deformation on parabolic cups drawn on (a) 1mm sheet and (b) 1.2mm sheet.

The strains obtained from the experiment are in good agreement with the strains obtained from simulation. The strains obtained from the simulation for 1 mm and 1.5 mm sheets are 2.49 and 2.38 respectively. Whereas the experimental strain of 1 mm thick parabolic was 2.11 and the strain of 1.5 mm parabolic cup was 1.7. When comparing simulation strains with the experimental strains, the strains obtained from the experiment are found to be on the lower side. This is because of absence of fracture in the experimentally formed cups. The strains obtained from simulation are higher because they represent the maximum values of rupture. This further indicates experimen-

tal strains are within the allowable limits of the formability of cup. Figure 11 shows the distribution of equivalent strain the formed cup.

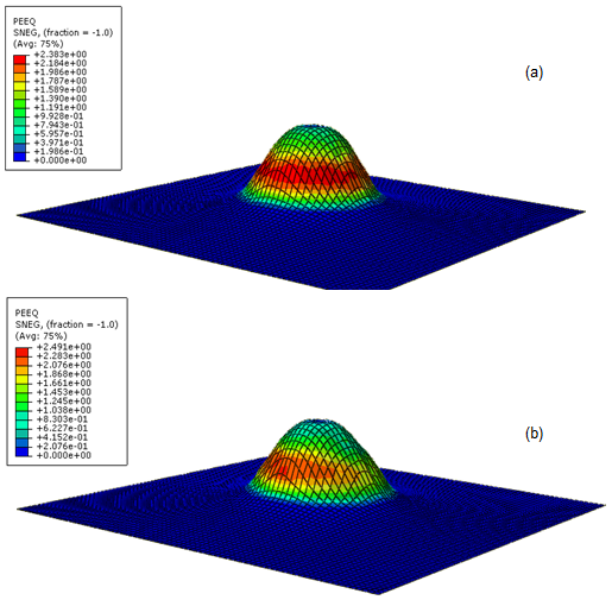

Fig. 11. Equivalent strain induced in (a) 1mm sheet and (b) 1.2mm sheet.

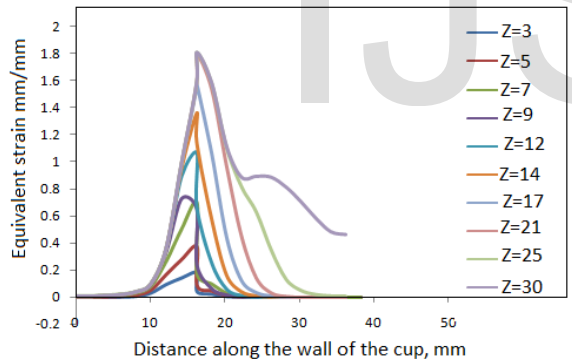

Fig. 12. Strain variation in the wall of the cup on 1mm thick sheet.

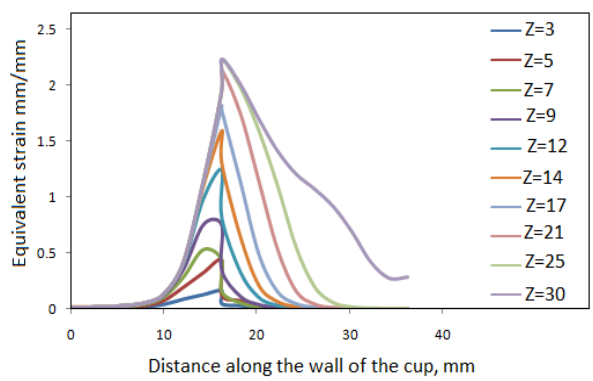

Fig. 13. Strain variation in the wall of the cup on 1.2mm thick sheet.

The strain variations along the wall of conical and pyramidal cups are shown in figures 12 and 13 respectively. It is observed that in the initial stages of forming the path of strain is almost linear and as the forming continues to take place the strain path follows a non-linear trend. The stress rises steeply up to 0.2 strain and later it remains constant even with increase in strain as shown in figure 14.

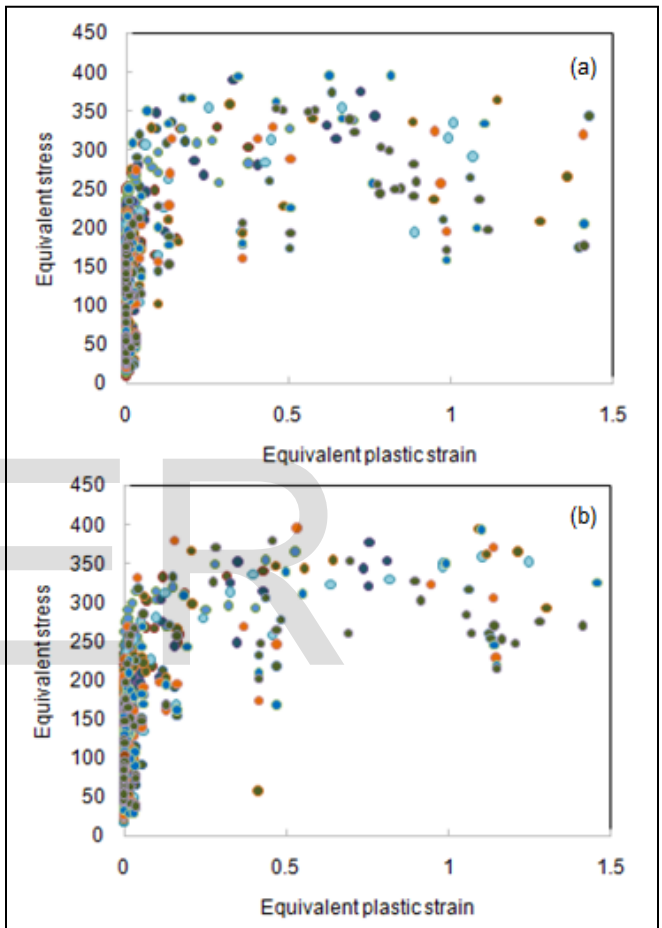

Fig. 14. Equivalent plastic strain vs equivalent stress for (a) 1mm and (b) 1.2mm thick sheets.

The thickness variations along the wall for 1 mm and 1.5 mm cup are shown in figure 15. The thickness variation along the walls followed the same trend as predicted by the simulation. It is the side walls of the cups which experienced the maximum reduction in thickness. This is due to the reason that; the side wall is the most strained part in the formed component as shown in figure 11. So, the elements in this part of the cup are more stretched when compare to other elements. The thickness reduction in the flange and the bottom of the cup was negligible.

Figure 16 represents the formability diagrams for the 1 mm and 1.5 mm parabolic cups. Both the cups follow the same pattern, which is; in the very initial stages of forming the compressive stresses are predominant. But in the later stages of

forming the formability limit diagrams of both the cups are dominated by the uni-axial tensile stress.

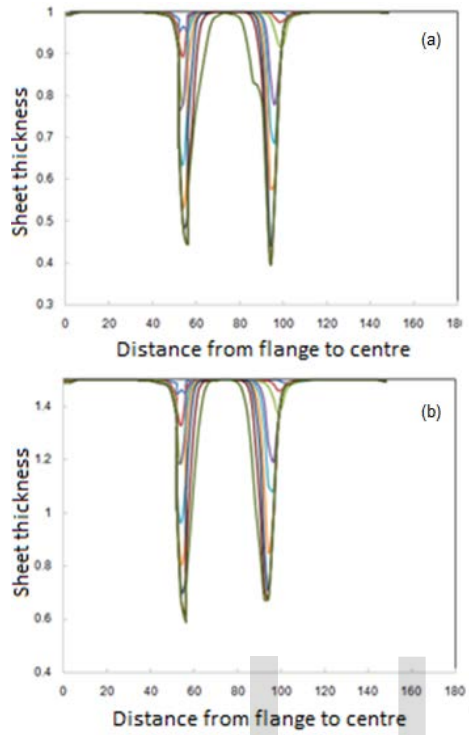

Fig. 15. Thickness variation along the walls of parabolic cup for (a) 1mm and (b) 1.2mm thick sheets.

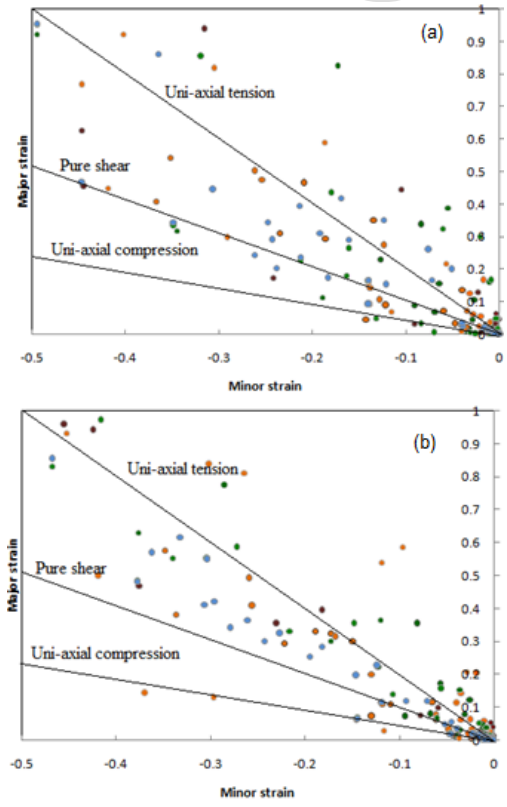

Fig. 16. Formability limit diagrams of (a) 1mm and (b) 1.2mm thick sheets.

4 Conclusion

In the present work, the finite element analysis and validation are successfully implemented for single point incremental forming process of AA6082 alloy sheet. It is found that the majority of thickness reduction takes place in the walls of the cup but not in the flange or bottom of the cup. The elements located at the mid regions of the walls are elongated higher than those present at the top and bottom of the cup. Though the initial formability of the parabolic cups is due to compressive stresses, the later stages of formability are dominated by tensile stresses. Experiments were conducted on CNC machine to verify the accuracy of simulated results. The experimental results were in good agreement with the simulated results. The stress pattern obtained on the formed cup was similar to that of the deformed pattern of mesh in simulated cups from FEA. The strain of the formed cup is within the limit of the formability.

Acknowledgment

The authors wish to thank UGC, New Delhi for financial assistance of this project.

References

[1] A. C. Reddy, Homogenization and Parametric Consequence of Warm Deep Drawing Process for 1050A Aluminum Alloy: Validation through FEA, International Journal of Science and Research, vol. 4, no. 4, pp. 2034-2042, 2015.
[2] A. C. Reddy, Formability of Warm Deep Drawing Process for AA1050-H18 Pyramidal Cups, International Journal of Science and Research, vol. 4, no. 7, pp. 2111-2119, 2015.
[3] A. C. Reddy, Formability of Warm Deep Drawing Process for AA1050-H18 Rectangular Cups, International Journal of Mechanical and Production Engineering Research and Development, vol. 5, no. 4, pp. 85-97, 2015.
[4] A. C. Reddy, Formability of superplastic deep drawing process with moving blank holder for AA1050-H18 conical cups, International Journal of Research in Engineering and Technology, vol. 4, no. 8, pp. 124-132, 2015.
[5] A. C. Reddy, Performance of Warm Deep Drawing Process for AA1050 Cylindrical Cups with and Without Blank Holding Force, International Journal of Scientific Research, vol. 4, no. 10, pp. 358-365, 2015.
[6] A. C. Reddy, Necessity of Strain Hardening to Augment Load Bearing Capacity of AA1050/AlN Nanocomposites, International Journal of Advanced Research, vol. 3, no. 6, pp. 1211-1219, 2015.
[7] A. C. Reddy, Parametric Optimization of Warm Deep Drawing Process of 2014T6 Aluminum Alloy Using FEA, International Journal of Scientific & Engineering Research, vol. 6, no. 5, pp. 1016-1024, 2015.
[8] A. C. Reddy, Finite Element Analysis of Warm Deep Drawing Process for 2017T4 Aluminum Alloy: Parametric Significance Using Taguchi Technique, International Journal of Advanced Research, vol. 3, no. 5, pp. 1247-1255, 2015.
[9] A. C. Reddy, Parametric Significance of Warm Drawing Process for 2024T4 Aluminum Alloy through FEA, International Journal of Science and Research, vol. 4, no. 5, pp. 2345-2351, 2015.
[10] A. C. Reddy, Formability of High Temperature and High Strain Rate Superplastic Deep Drawing Process for AA2219 Cylindrical Cups, International Journal of Advanced Research, vol. 3, no. 10, pp. 1016-1024, 2015.
[11] C. R Alavala, High temperature and high strain rate superplastic deep drawing process for AA2618 alloy cylindrical cups, International Journal of Scientific Engineering and Applied Science, vol. 2, no. 2, pp. 35-41, 2016.

[12] C. R Alavala, Practicability of High Temperature and High Strain Rate Superplastic Deep Drawing Process for AA3003 Alloy Cylindrical Cups, International Journal of Engineering Inventions, vol. 5, no. 3, pp. 16-23, 2016.
[13] C. R Alavala, High temperature and high strain rate superplastic deep drawing process for AA5049 alloy cylindrical cups, International Journal of Engineering Sciences & Research Technology, vol. 5, no. 2, pp. 261-268, 2016.
[14] C. R Alavala, Suitability of High Temperature and High Strain Rate Superplastic Deep Drawing Process for AA5052 Alloy, International Journal of Engineering and Advanced Research Technology, vol. 2, no. 3, pp. 11-14, 2016.
[15] C. R Alavala, Development of High Temperature and High Strain Rate Super Plastic Deep Drawing Process for 5656 Al- Alloy Cylindrical Cups, International Journal of Mechanical and Production Engineering, vol. 4, no. 10, pp. 187-193, 2016.
[16] C. R Alavala, Effect of Temperature, Strain Rate and Coefficient of Friction on Deep Drawing Process of 6061 Aluminum Alloy, International Journal of Mechanical Engineering, vol. 5, no. 6, pp. 11-24, 2016.
[17] A. C. Reddy, Finite element analysis of reverse superplastic blow forming of Ti-Al-4V alloy for optimized control of thickness variation using ABAQUS, Journal of Manufacturing Engineering, National Engineering College, vol. 1, no. 1, pp. 6-9, 2006.
[18] A. C. Reddy, T. Kishen Kumar Reddy, M. Vidya Sagar, Experimental characterization of warm deep drawing process for EDD steel, International Journal of Multidisciplinary Research & Advances in Engineering, vol. 4, no. 3, pp. 53-62, 2012.
[19] A. C. Reddy, Evaluation of local thinning during cup drawing of gas cylinder steel using isotropic criteria, International Journal of Engineering and Materials Sciences, vol. 5, no. 2, pp. 71-76, 2012.
[20] C. R Alavala, Fem Analysis of Single Point Incremental Forming Process and Validation with Grid-Based Experimental Deformation Analysis, International Journal of Mechanical Engineering, 5, 5, 1-6, 2016.
[21] C. R Alavala, Validation of Single Point Incremental Forming Process for Deep Drawn Pyramidal Cups Using Experimental Grid-Based Deformation, International Journal of Engineering Sciences & Research Technology, vol. 5, no. 8, pp. 481-488, 2016.
[22] M. Azaouzi, N. Lebaal, Tool path optimization for single point incremental sheet forming using response surface method, Simul Model Pract Theor, vol. 24, pp. 49–58, 2012.
[23] L. Filice, L. Fratini, F. Micari, Analysis of material formability in incremental forming, CIRP Ann Manuf Technol, vol. 51, no. 1, pp. 199–202, 2002.
[24] S. Thibaud, R. B. Hmida, F. Richard, P. Malecot, A fully parametric toolbox for the simulationof single point incremental sheet forming process: numerical feasibility and experimental validation, Simulation Modeling Practice Theory, vol. 29, pp. 42–43, 2012.
[25] D.M Neto et.al. Evaluation of strain and stress states in the single point incremental forming process, The International Journal of Advanced Manufacturing Technology, vol. 85, page 521-534.
[26] S. D Majagi, G. Chandramohan, M. Senthil Kumar, Effect of incremental forming process parameters on aluminum alloy using experimental studies, Advanced Materials Research, vol. 1119, No. 2, pp 633-639, 2015.
[27] H. Arfa, R. Bahloul, H. Bel Hadj SalahFinite element modelling and experimental investigation of single point incremental forming process of aluminium sheets: influence of process parameters on punch force monitoring and on mechanical and geometrical quality of parts, International Journal of Material Forming, No. 6, pp. 483–510, 2013.
[28] C. R. Alavala, Finite element methods: Basic Concepts and Applications, PHI Learning Pvt. Ltd., 2008.
[29] C. R. Alavala, CAD/CAM: Concepts and Applications, PHI Learning Pvt. Ltd, 2008.